PHYSICAL REVIEW B VOLUME 33, NUMBER 2 15 JANUARY 1986

Electron charge densities at conduction-band edges of semiconductors

Steven L. Richardson and Marvin L. Cohen
Department of Physics, University of California, and Center for Advanced Materials,
Lawrence Berkeley Laboratory, Berkeley, California 94720

Steven G. Louie
Department of Physics, University of California, and Materials and Molecular Research Division,
Lawrence Berkeley Laboratory, Berkeley, California 94720

James R. Chelikowsky
Corporate Research-Science Laboratories, Exxon Research and Engineering Company,
Clinton Township, Rt. 22 East, Annandale, New Jersey 08801

(Received 13 May 1985)

We demonstrate that both the empirical pseudopotential method (EPM) and the linear combination of atomiclike orbitals (LCAO) approach are capable of producing consistent electronic charge distributions in a compound semiconductor. Since the EPM approach is known to produce total valence electron charge densities which compare well with experimental x-ray data (e.g., Si), this work serves as a further test for the LCAO method. In particular, the EPM scheme, which uses an extended plane-wave basis, and the LCAO scheme, which employs a localized Gaussian basis, are used, with the *same* empirical potential as input, to analyze both the total valence electron charge density and the charge density of the first conduction band at the Γ, *L*, and *X* **k** points of the Brillouin zone. These charge densities are decomposed into their *s*-, *p*-, and *d*-orbital contributions, and this information is used to interpret the differences in the topologies of the conduction bands at Γ, *L*, and *X*. Such differences are crucial for a comprehensive understanding of interstitial impurities and the response of specific band states to perturbations in compound semiconductors.

I. INTRODUCTION

The theoretical and experimental study of electronic charge densities in atoms, molecules, and solids is of fundamental interest to researchers in the material sciences. By first solving the Schrödinger wave equation in the single-particle picture to obtain the wave function $\psi(\mathbf{r})$ of a particular quantum-mechanical system, one can subsequently calculate the electron charge probability density

$$\rho(\mathbf{r})=e\,|\,\psi(\mathbf{r})\,|^2 \qquad (1)$$

for locating an electron of charge e in a given region. When this prescription was first applied to the hydrogen molecule,[1] it was discovered that the electronic charge-density profile for H_2 strongly depended on the particular energy state under question. For example, the ground state or bonding orbital σ consisted of a charge contour with a substantial amount of electronic charge density between the nuclei, thus fostering a strong chemical bond, whereas the antibonding orbital σ^* was characterized by a nodal plane between the two nuclei making the system unstable relative to the bonding orbital. Since that time, the electronic charge-density distribution in more complicated molecular systems has been explored in greater detail by generations of chemists, and these studies have substantially increased our understanding of molecular geometries,[2] bonding properties,[3] and reaction mechanisms of molecular processes.[4]

The problem of studying charge densities in crystalline solids is more involved since the periodicity of the crystal gives the wave function $\psi(\mathbf{r})$ both an energy-band and a wave-vector dependence, $\psi_{n,\mathbf{k}}(\mathbf{r})$, denoted by n and $\mathbf{k}$, respectively. The electronic charge density $\rho(\mathbf{r})$ is now obtained from summing over all the occupied $\mathbf{k}$ states of the crystal of the occupied bands n,

$$\rho(\mathbf{r})=2e\sum_{n,\mathbf{k}}^{\text{occ}}|\,\psi_{n,\mathbf{k}}(\mathbf{r})\,|^2\,. \qquad (2)$$

One of the earliest attempts to obtain accurate charge-density distributions in semiconductors was made by Walter and Cohen.[5] They used the empirical pseudopotential method[6–11] (EPM) to calculate a pseudo-wave-function $\psi_{n,\mathbf{k}}(\mathbf{r})$ which described the valence electrons of the semiconductor, and computed the total valence electron charge density $\rho(\mathbf{r})$ by summing over all available $\mathbf{k}$ states for the occupied valence bands of the semiconductor. In a further study,[12] Walter and Cohen used the EPM scheme to analyze the electronic charge densities in semiconductors as a function of particular band index, $\rho_n(\mathbf{r})$, where

$$\rho_n(\mathbf{r})=2e\sum_{\mathbf{k}}|\,\psi_{n,\mathbf{k}}(\mathbf{r})\,|^2\,, \qquad (3)$$

and thus provided some qualitative insight into bonding trends. They discovered that in some cases the charge densities at the valence and conduction bands of semiconductors bore a resemblance to the bonding and antibonding orbital configurations found in molecules.

In addition to the band index, the charge density at a specific **k** point of a given band, $\rho_{n,\mathbf{k}}(\mathbf{r})$, can also be obtained. Calculations were performed for several semiconductors,[13] but results were reported only for selected **k** points in Ge.[8] A more complete study is warranted since a knowledge of $\rho_{n,\mathbf{k}}(\mathbf{r})$ is useful in understanding the effect of impurities on the electronic band structure of semiconductors and, more generally, the response of specific states to perturbations.

In this paper we use two different methods to study the electronic charge density $\rho_{n,\mathbf{k}}(\mathbf{r})$ at the Γ, L, and X **k** points of the first conduction band of GaAs: the empirical pseudopotential method (EPM) with nonlocal pseudopotentials,[9] which has been successful in computing total valence electron charge densities that have, for example, been verified experimentally for Si;[14] and the linear combination of atomiclike orbitals (LCAO) method of Chelikowsky and co-workers[15,16] which has been recently applied to a variety of problems including cohesive and structural properties,[15] surface reconstructions,[17] and phonon-phonon interactions in diamond.[18] For consistent comparison, the same empirical potential is utilized as input in the two approaches used in the present study. These two methods differ rather dramatically in that the EPM scheme uses a nearly-free-electron approach since it employs an extended plane-wave basis to describe the wave functions of the system, while the LCAO method implements localized Gaussian-type orbitals as a basis set and is therefore similar to many quantum chemical approaches used in studying tightly bound electronic systems such as molecules and clusters.

We first construct a crystal potential for GaAs which is used as input for both the EPM and LCAO calculations (Sec. II). The choice of a basis set in each method and the diagonalization of their respective secular equations for obtaining eigenvalues and wave functions are described in Sec. III. In Sec. IV these two approaches are used to compute a band structure for GaAs and both the total valence electron charge density and electron charge densities of the first conduction band at the Γ, L, and X **k** points. These charge densities at selected **k** points are then decomposed into their s-, p-, and d-orbital contributions, and the information is used to analyze the observed differences among the charge-density topologies at the Γ, L, and X **k** points. Finally, our conclusions are summarized in Sec. V.

II. CONSTRUCTION OF MODEL POTENTIAL

To compare the EPM and LCAO schemes for calculating the electronic charge densities at selected **k** points in the Brillouin zone of a given semiconductor, one must utilize the same input parameters for both calculations. We, therefore, construct a model total potential for the crystal which serves as input for both schemes. Consequently, the major difference between the two calculations will be the choice of basis (i.e., plane waves or localized Gaussians).

To construct a model potential for the LCAO calculation, we fixed a potential $V^a(\mathbf{r})$ for each atom

$$V^a(\mathbf{r})=\sum_i a_i e^{-b_i r^2} \tag{4}$$

by comparing it to the potential used in a previous EPM calculation by Chelikowsky and Cohen,[9] where a_i and b_i are the coefficient and decay constant of the ith Gaussian, respectively. It was necessary to include five Gaussians for the arsenic atom and six Gaussians for the gallium atom in Eq. (4), and the coefficients and decay constants are listed in Table I. The total model potential for the LCAO calculation is then computed by summing over all of the atomic sites of the crystal.

TABLE. I. Coefficients (in Ry) and decay constants (in a.u.) for Gaussian expansion of the model potentials in real space.

a_i	b_i
Ga	
−12.91	0.1597
0.13	0.1882
58.35	0.2083
−100.23	0.2795
56.30	0.3592
−0.35	0.4000
As	
−10.44	0.1540
0.63	0.1882
48.66	0.2015
−98.07	0.2771
60.37	0.3469

The same input model potential was constructed for the EPM calculation by analytically Fourier-transforming these atomic potentials $V^a(\mathbf{r})$ into momentum space and thus obtaining a set of pseudopotential form factors $V(\mathbf{G})$ as discussed previously.[9] The symmetric and antisymmetric pseudopotential form factors which we obtained are listed in Table II, and differ slightly from those in Ref. 9 because of the inclusion of the tail in the potential $V(\mathbf{G})$ for $\mathbf{G}^2>11$, which slightly readjusts the form factors at lower values of momentum.

Finally, we should mention that the pseudopotential is nonlocal, and this is explicitly included in both methods. The Chelikowsky-Cohen nonlocal pseudopotential scheme[9] was used for the EPM calculation, while, in the LCAO approach, the nonlocal contribution to the poten-

TABLE II. Pseudopotential form factors for GaAs (in Ry) as determined from the model potentials. Those form factors whose structure factors vanish by symmetry are not shown.

$\lvert\mathbf{G}\rvert$ (in units of $2\pi/a$)	V^S	V^A
$\sqrt{3}$	−0.2271	+0.0419
$\sqrt{4}$		+0.0273
$\sqrt{8}$	+0.0110	
$\sqrt{11}$	+0.0631	−0.0014
$\sqrt{12}$		−0.0011
$\sqrt{16}$	+0.0535	
$\sqrt{19}$	+0.0357	−0.0009

tial for each atom was modeled following Chelikowsky and Louie,[15] where the *d* potential is chosen as the local potential, for convenience, while the nonlocal contribution is defined so that the *total* LCAO potential is exactly the same as that of the EPM potential for all angular momentum components $l \leq 2$.

III. CHOICE OF BASIS AND SOLUTION OF SCHRÖDINGER EQUATION

As previously stated, the major difference between the EPM and LCAO approaches in calculating the electronic properties of solids rests in the selection of the basis set. The EPM scheme employs an extended plane-wave basis where the pseudo-wave-function is expressed as an expansion over an arbitrarily large number of plane waves[6-11]

$$\psi_{n,\mathbf{k}}(\mathbf{r})=\sum_{\mathbf{G}}\psi_n(\mathbf{k}+\mathbf{G})e^{i(\mathbf{k}+\mathbf{G})\cdot\mathbf{r}} , \qquad (5)$$

where in our calculation the expansion is cut off at 8 Ry, thus including 113 plane waves. While this method is conceptually simpler than the LCAO approach, it may require a large number of plane waves for reliable results in cases where electrons are more localized about the ions.

On the other hand, the LCAO method uses a Bloch sum of Gaussian orbitals of *s*-, *p*-, and *d*-like symmetry as a basis set. The selection process for the decay constants β of the local orbitals has been described elsewhere for the case of diamond.[15] For GaAs, we used three decay constants ($\beta_1=0.15$, $\beta_2=0.30$, $\beta_3=0.60$) for each of the 10 orbitals ($s,p_x,p_y,p_z,d_{xy},d_{yz},d_{zx},d_{x^2-y^2},d_{3z^2-1},r^2s$) giving a total of 30 Gaussian orbitals per atom. Using this basis the secular equation is solved. The Hamiltonian matrix elements are conveniently evaluated in real space as opposed to momentum space as in the EPM scheme,[6-11] and the matrix equation to be diagonalized is smaller. A value of 14 a.u. was chosen for the real-space cutoff parameter $\mathbf{R}_{\max}$ which is required for the evaluation of matrix elements in the LCAO program.[15]

IV. RESULTS

A. Band structure for GaAs

Using the model potential and basis sets described in Secs. II and III, respectively, we first calculate the band structure of GaAs using both the EPM and LCAO approaches. The eigenvalues for GaAs at selected symmetry points are shown in Table III where spin-orbit corrections have been neglected. The two methods yield eigenvalues which are in good agreement. In particular, the eigenvalues in the first conduction band agree to within 0.2 eV. We also find that our calculated eigenvalues agree well with the experimentally measured bands[19] with the possible exception of the lowest band, which is the one whose position is the most difficult to determine experimentally because of secondary-emission effects.

B. Charge-density calculations

The wave functions $\psi_{n,\mathbf{k}}(\mathbf{r})$ obtained from solving the secular equations of the EPM and LCAO schemes are

TABLE III. Eigenvalues (in units of eV referred to the valence-band maximum) for GaAs at three **k** points using the EPM and LCAO approaches. Also shown are measured angle-resolved photoemission spectroscopy eigenvalues of conduction and valence bands (Ref. 19). Spin-orbit interactions are not included.

	EPM	LCAO	Experimental[a]
Γ_1^v	−12.26	−12.26	−13.1
Γ_{15}^v	+0.00	+0.00	+0.00
Γ_1^c	+1.55	+1.69	+1.63
Γ_{15}^c	+4.60	+4.89	+4.72
L_1^v	−10.27	−10.32	−11.24
L_1^v	−6.78	−6.80	−6.70
L_3^v	−1.22	−1.10	−1.30
L_1^c	+1.86	+1.95	+1.85
L_3^c	+5.67	+5.85	
X_1^v	−9.36	−9.43	−10.75
X_3^v	−7.06	−7.06	−6.70
X_5^v	−2.77	−2.60	−2.80
X_1^c	+2.53	+2.47	+2.18
X_3^c	+2.56	+2.53	+2.58

[a] Reference 19.

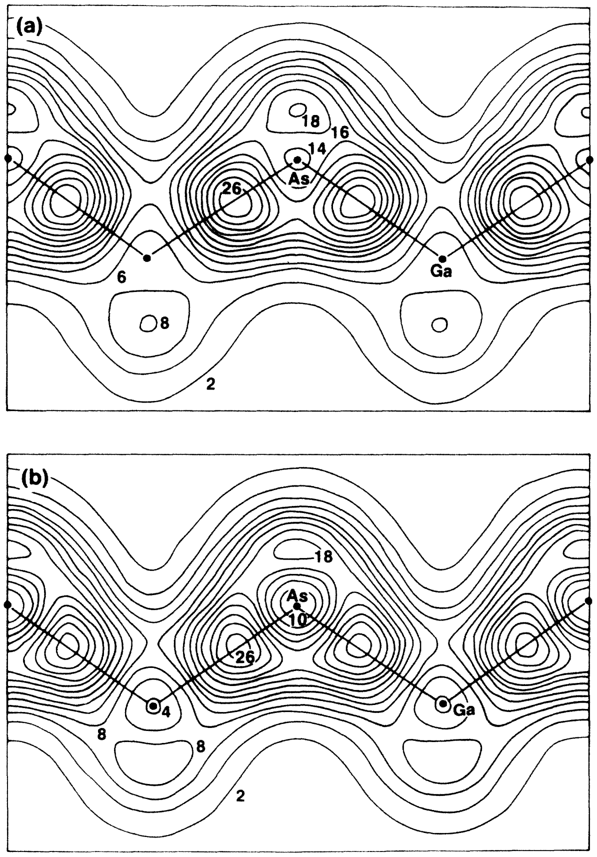

FIG. 1. Total valence electron charge-density contours for GaAs in the $(1\bar{1}0)$ plane using (a) EPM and (b) LCAO schemes. The contour interval for both plots is in units of 2.0 electrons per primitive cell.

employed to compute the total valence electron charge density $\rho(\mathbf{r})$ given in Eq. (2). The sum over $\mathbf{k}$, which in principle extends over the entire Brillouin zone, is reduced to a sum over the irreducible part[20] and then computed for two special $\mathbf{k}$ points, $(2\pi/a)(\frac{1}{4},\frac{1}{4},\frac{1}{4})$ and $(2\pi/a)(\frac{1}{4},\frac{1}{4},\frac{3}{4})$, using the Chadi-Cohen scheme.[21] The total valence charge density is obtained by summing over the four occupied valence bands. The results are shown in Fig. 1 where the agreement between the two plots is quite good, with the only discernable discrepancy being some extra contours close to the nuclei. Nevertheless, both methods faithfully reproduce the sp^3 covalent-bonding orbital along the Ga-As bonding chain with most of the charge density shifted towards the As ion.

To compute the charge density at a specific $\mathbf{k}$ point in a given band n, we evaluate $\rho_{n,\mathbf{k}}(\mathbf{r})$ as

$$\rho_{n,\mathbf{k}}(\mathbf{r})=e\,|\,\psi_{n,\mathbf{k}}(\mathbf{r})\,|^2\,. \qquad (6)$$

Shown in Figs. 2, 3, and 4 are both the EPM- and LCAO-generated electron charge densities in the $(1\bar{1}0)$ plane of GaAs at the Γ, L, and X $\mathbf{k}$ points of the first conduction band. Apart from some minor differences in the charge densities near the nuclei, both methods reveal that the charge densities at Γ and L are concentrated about the ions, while the charge distribution at X is more uniformly distributed.

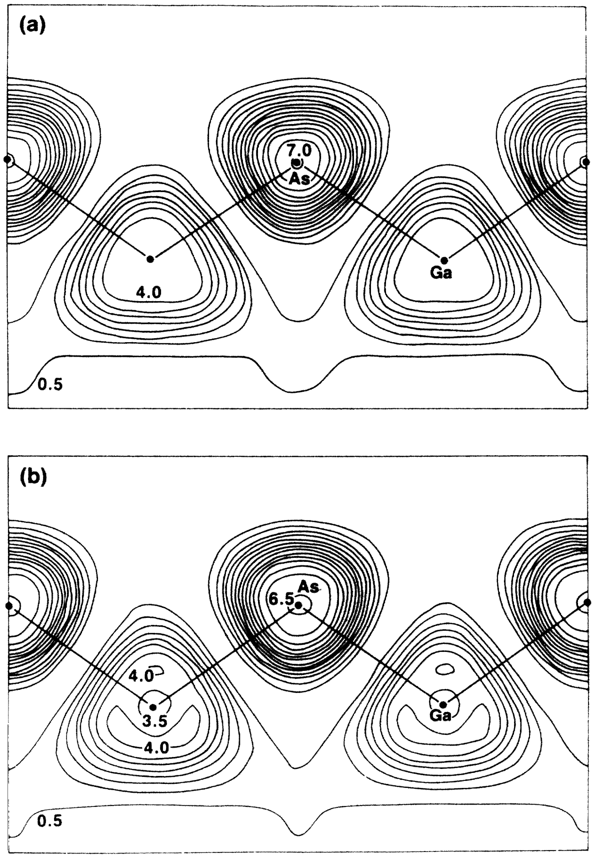

FIG. 2. Electron charge-density contours for GaAs in the $(1\bar{1}0)$ plane at the Γ point of the first conduction band using (a) EPM and (b) LCAO schemes. The contour interval for both plots is in units of 0.5 electron per primitive cell.

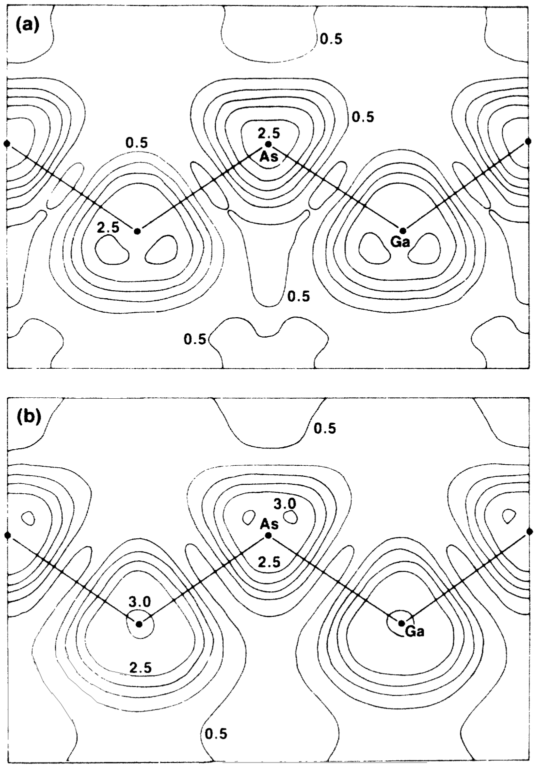

FIG. 3. Electron charge-density contours for GaAs in the $(1\bar{1}0)$ plane at the L point of the first conduction band using (a) EPM and (b) LCAO schemes. The contour interval for both plots is in units of 0.5 electron per primitive cell.

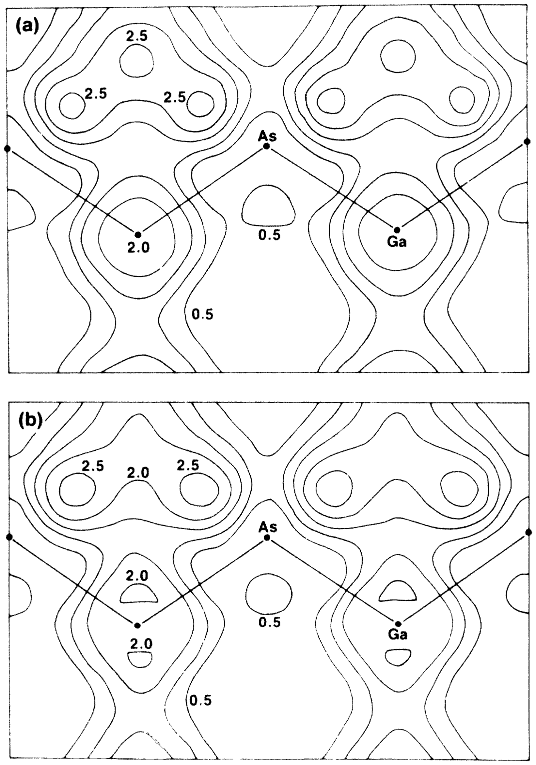

FIG. 4. Electron charge-density contours for GaAs in the $(1\bar{1}0)$ plane at the X point of the first conduction band using (a) EPM and (b) LCAO schemes. The contour interval for both plots is in units of 0.5 electron per primitive cell.

TABLE IV. Percentage decomposition of angular momentum character for wave functions of the first conduction band of GaAs.

GaAs	s	p_x	p_y	p_z	d_{xy}	d_{yz}	d_{zx}	$d_{x^2-y^2}$	d_{3z^2-1}
Γ									
Ga	49								
As	51								
L									
Ga	31		← 11 →			← 12 →			
As	20		← 7 →			← 19 →			
X [(001)$2\pi/a$]									
Ga	22								25
As				17	36				

To understand better the differences among these distributions, the wave functions at the Γ, L, and X **k** points of the first conduction band were decomposed into their s-, p-, and d-orbital contributions. Since we have demonstrated that there is little difference between the charge densities calculated from either the LCAO or EPM approach, the EPM wave functions were chosen for decomposition because of the simplicity of their plane-wave basis.

The angular momentum contribution of the electron charge density within a Wigner-Seitz sphere centered on a particular atomic site, $\chi_{l,m}^{\tau_j,n,\mathbf{k}}$, can be calculated from the expression[22]

$$\chi_{l,m}^{\tau_j,n,\mathbf{k}}=4\pi\int_0^R r^2dr\langle\psi_{n,\mathbf{k}}\,|\,Y_{l,m}\rangle\langle Y_{l,m}\,|\,\psi_{n,\mathbf{k}}\rangle\ , \qquad (7)$$

where R is the Wigner-Seitz radius and $Y_{l,m}$ is the spherical harmonic function. By normalizing this quantity with the total contribution from the other angular momentum components for both atoms, the percentage decomposition of s, p, and d character of the eigenfunction at a particular **k** point is easily computed. Equation (7) has been numerically evaluated at the Ga and As sites. The results are illustrated in Table IV.

Upon comparing these results with Figs. 2, 3, and 4, we observe that the charge distribution at Γ is antibonding-like with a nodal plane intersecting the internuclear axis connecting the Ga and As ions. This charge distribution is also predominantly s-like[23] with most of the charge localized on the anion.[24] The charge density at L is quite similar to that at Γ except that it contains more p and d character ($p_x,p_y,p_z,d_{xy},d_{yz},d_{zx}$), and is more uniformly localized on the cation (Ga) and anion (As). The situation at X, however, is dramatically different since it contains a significantly higher d contribution ($d_{xy},d_{yz},d_{zx},d_{3z^2-1}$) and is more free-electron-like with a slight abundance of charge about the cation. Such differences have also been discussed by Bachelet and Christensen[25] using a relativistic linear muffin-tin orbital calculation on GaAs, but in a much more qualitative manner. There is also an enhancement of electron charge density in the interstitial region at X which is relevant when considering the effect of interstitial impurities on the electronic band structure of elemental and compound semiconductors.[25,26]

Finally, we should also remark that our results are consistent with group-theoretical predictions.[27]

V. CONCLUSION

In this work, we demonstrate the ability of two calculational procedures, the EPM and LCAO schemes, to study electronic charge-density distributions in semiconductors (e.g., GaAs). Although these methods use entirely different types of wave functions as their basis sets [i.e., extended plane-wave (EPM) and localized Gaussian orbitals (LCAO)], they produce consistent electronic charge-density distributions both at selected **k** points in the Brillouin zone (e.g., Γ, L, and X **k** points of the first conduction band) and for the total valence electron charge density using the Chadi-Cohen special **k** point scheme. These charge distributions are decomposed into their s, p, and d wave-function contributions, and their antibonding topologies are analyzed both numerically and group-theoretically. These results, therefore, yield useful information about interstitial impurities and the response of specific band states to perturbations in compound semiconductors.

ACKNOWLEDGMENTS

We are grateful to Mark S. Hybertsen for many enlightening conversations on the EPM computer codes and to Che-ting Chan for his expert assistance in fitting the EPM form factors to Gaussians and his discussions on the angular momentum decomposition program. We also acknowledge conversations with KeeJoo Chang, Mei-Yin Chou, Michel M. Dacorogna, Sverre Fröyen, and Pui K. Lam. One of us (S.L.R.) is particularly appreciative of many helpful discussions on group theory with Professor Leo Falicov, Professor Conyers Herring, Professor Charles Kittel, and Dr. James Phillips, and wishes to thank the Chancellor's Office of the University of California at Berkeley for financial support. Support for this work was provided by National Science Foundation Grant No. DMR8319024 and by the Director, Office of Energy Research, Office of Basic Energy Sciences, Materials Sciences Division of the U.S. Department of Energy under Contract No. DE-AC03-76SF00098.

[1] W. Heitler and F. London, Z. Phys. **44**, 455 (1927); F. Hund, Trans. Faraday Soc. **25**, 646 (1929); J. E. Lennard-Jones, *ibid.* **25**, 668 (1929); R. S. Mulliken, Phys. Rev. **41**, 49 (1932).

[2] J. A. Campbell, *Chemical Systems: Energetics, Dynamics, Structure* (Freeman, San Francisco, 1970); R. E. Dickerson, H. B. Gray, and G. P. Haight, Jr., *Chemical Principles* (Benjamin, New York, 1970).

[3] L. Pauling, *The Nature of the Chemical Bond,* 3rd ed. (Cornell University Press, Ithaca, 1960).

[4] See, for example, R. C. D. Breslow, *Organic Reaction Mechanisms: An Introduction,* 2nd ed. (Benjamin, New York, 1969).

[5] J. P. Walter and M. L. Cohen, Phys. Rev. Lett. **26**, 17 (1971); M. L. Cohen, Science **179**, 1189 (1979).

[6] M. L. Cohen and T. K. Bergstresser, Phys. Rev. **141**, 789 (1966).

[7] M. L. Cohen and V. Heine, in *Solid State Physics,* edited by H. Ehrenreich, F. Seitz, and D. Turnbull (Academic, New York, 1970), Vol. 24, p. 37.

[8] J. C. Phillips, *Bond and Bands in Semiconductors* (Academic, New York, 1976).

[9] J. R. Chelikowsky and M. L. Cohen, Phys. Rev. **14**, 556 (1976).

[10] J. C. Phillips, Phys. Rev. **112**, 685 (1958).

[11] F. Bassani and V. Celli, J. Phys. Chem. Solids **20**, 64 (1961).

[12] J. P. Walter and M. L. Cohen, Phys. Rev. B **4**, 1877 (1971).

[13] J. P. Walter and M. L. Cohen (private communication).

[14] Y. W. Yang and P. Coppens, Solid State Commun. **15**, 1555 (1974).

[15] J. R. Chelikowsky and S. G. Louie, Phys. Rev. B **29**, 3470 (1984).

[16] J. R. Chelikowsky, S. G. Louie, D. Vanderbilt, and C. T. Chan, Int. J. Quant. Chem. Symp. **18**, 105 (1984).

[17] D. Vanderbilt and S. G. Louie, Phys. Rev. B **30**, 6118 (1984).

[18] D. Vanderbilt, S. G. Louie, and M. L. Cohen, Phys. Rev. Lett. **53**, 1477 (1984).

[19] T.-C. Chiang, J. A. Knapp, M. Aono, and D. E. Eastman, Phys. Rev. B **21**, 3513 (1980).

[20] M. Schlüter, G. Martinez, and M. L. Cohen, Phys. Rev. B **11**, 3808 (1975).

[21] D. J. Chadi and M. L. Cohen, Phys. Rev. B **8**, 5747 (1973).

[22] See, for example, C. T. Chan and S. G. Louie, Phys. Rev. B **27**, 3325 (1983); P. K. Lam and M. L. Cohen, *ibid.* **27**, 5986 (1983).

[23] We have ignored the contribution of f orbitals in our angular momentum decomposition, although group theory suggests a nonzero contribution of f-orbital character. Hence, strictly speaking, the charge distribution is not purely s-like.

[24] A. Baldereschi and K. Maschke, in *Proceedings of the 14th International Conference on the Physics of Semiconductors, Edinburgh, 1978,* edited by B. L. H. Wilson (IOP, Bristol, 1978), p. 1167.

[25] G. B. Bachelet and N. E. Christensen, Phys. Rev. B **31**, 879 (1985).

[26] H. W. A. M. Rompa, M. F. H. Schuurmans, and F. Williams, Phys. Rev. Lett. **52**, 675 (1984); D. M. Wood, A. Zunger, and R. de Groot, Phys. Rev. B **31**, 2570 (1985); S. L. Richardson, M. L. Cohen, S. G. Louie, and J. R. Chelikowsky, Phys. Rev. Lett. **54**, 2549 (1985).

[27] See, for example, F. Bassani and G. Pastori Parravicini, *Electronic States and Optical Transitions in Solids* (Pergamon, Oxford, 1975); F. A. Cotton, *Chemical Applications of Group Theory,* 2nd ed. (Wiley-Interscience, New York, 1971); M. Tinkham, *Group Theory and Quantum Mechanics* (McGraw-Hill, New York, 1964); F. Bassani, in *Semiconductors and Semimetals,* edited by R. K. Willardson and A. C. Beer (Academic, New York, 1966).